J. Membrane Biol. 76, 139–149 (1983)

The Journal of
Membrane Biology

Thermotropic Lipid Phase Separations in Human Platelet and Rat Liver Plasma Membranes

Larry M. Gordon*, Patrick W. Mobley**, Judy A. Esgate*, Gary Hofmann**, Anthony D. Whetton +, and Miles D. Houslay +

* Rees-Stealy Research Foundation, San Diego, California 92101
** Department of Chemistry, California State Polytechnic University, Pomona, California 91768, and
\+ Department of Biochemistry and Molecular Biology, University of Manchester Institute of Science and Technology, Manchester M60 1QD, United Kingdom

Summary. Electron spin resonance (ESR) studies were conducted on human platelet plasma membranes using 5-nitroxide stearate, I(12,3). The polarity-corrected order parameter S and polarity-uncorrected order parameters $S(T_\parallel)$ and $S(T_\perp)$ were independent of probe concentration at low I(12,3)/membrane protein ratios. At higher ratios, S and $S(T_\perp)$ decreased with increasing probe concentration while $S(T_\parallel)$ remained unchanged. This is the result of enhanced radical interactions due to probe clustering. A lipid phase separation occurs in platelet membranes that segregates I(12,3) for temperatures less than 37 °C. As Arrhenius plots of platelet acid phosphatase activity exhibit a break at 35 to 36 °C, this enzyme activity may be influenced by the above phase separation. Similar experiments were performed on native [cholesterol/phospholipid ratio (C/P) = 0.71] and cholesterol-enriched [C/P = 0.85] rat liver plasma membranes. At 36 °C, cholesterol loading reduces I(12,3) flexibility and decreases the probe ratio at which radical interactions are apparent. The latter effects are attributed to the formation of cholesterol-rich lipid domains, and to the inability of I(12,3) to partition into these domains because of steric hinderance. Cholesterol enrichment increases both the high temperature onset of the phase separation occurring in liver membranes from 28° to 37 °C and the percentage of probe-excluding, cholesterol-rich lipid domains at elevated temperatures. A model is discussed attributing the lipid phase separation in native liver plasma membranes to cholesterol-rich and -poor domains. As I(12,3) behaves similarly in cholesterol-enriched liver and human platelet plasma membranes, cholesterol-rich and -poor domains probably exist in both systems at physiologic temperatures.

Key Words platelet plasma membranes · liver plasma membranes · spin probe · cholesterol · lipid phase separation · platelet acid phosphatase

Introduction

Recent studies suggest that lipid domains of differing structure and composition coexist in biological membranes, even at physiologic temperatures [5, 12, 22]. Indeed, cholesterol has been shown to be distributed nonrandomly in a variety of cell plasma membranes [9, 15]. The existence of cholesterol-rich and -poor lipid domains is consistent with the finding that specific phospholipids may achieve a lateral segregation of cholesterol in the bilayer [7]. Such inhomogeneous lipid distributions may well be responsible for those restricted lipid domains previously identified in surface membranes [6, 13, 28, 32].

The nature of temperature-dependent lipid phase separations in either rat liver plasma membranes or human platelet plasma membranes is investigated here using the 5-nitroxide stearate spin probe, I(12,3). A lipid phase separation between 28° and 19 °C can be detected in native rat liver plasma membranes by several physical methods, including spin-label techniques [*see*, for review, Refs. 12, 17]. As cholesterol is present in rat liver plasma membranes at concentrations [33] that in model systems smear out lipid phase transitions [7, 23], we suggested that for lipid phase separations to occur there must be areas of the bilayer that are cholesterol-free [14, 17, 19]. In the present spin-label study, the role that cholesterol plays in this lipid phase separation is examined by enriching liver membranes with sterol [33]. We also explore the possibility that a temperature-dependent lipid phase separation occurs in another cholesterol-rich biomembrane, human platelet plasma membranes.

Materials and Methods

Materials

The N-oxyl-4′,4′-dimethyloxazolidine derivative of 5-keto-stearic acid, I(12,3), was obtained from Syva Co., Palo Alto, Calif. All other chemicals and reagents were from Sigma Chemical Co., St. Louis, Mo.

Preparation of Native and Cholesterol-Enriched Rat Liver Plasma Membranes

Liver plasma membranes were isolated from male Sprague-Dawley rats weighing between 200 and 300 g as described before [18]. Cholesterol enrichment was performed by incubating membranes with cholesterol-rich liposomes, and cholesterol and phospholipid determinations were as set out earlier [33].

Preparation and Characterization of Human Platelet Plasma Membranes

Human platelet plasma membranes were purified according to the method of Barber and Jamieson [1], with several modifications. All subsequent procedures were approved by Human Subjects Review Committees at Scripps Clinic and Research Foundation and Rees-Stealy Research Foundation. Two to three units of blood, anticoagulated with citrate-phosphate-dextrose, were obtained from a commercial blood bank and kept at room temperature. A platelet-rich suspension, prepared as in Sauerheber *et al.* [29], was applied to 0 to 4.3 M glycerol gradients that were formed in centrifuge tubes with a Buchler triple-outlet gradient maker. These tubes were centrifuged in a Beckman SW-27.1 rotor at $1{,}460 \times g$ for 30 min, and then at $5{,}800 \times g$ for 10 min. Glycerol-loaded platelets in the pellet were lysed by addition of 50 mM Tris-HCl, 8% (wt/vol) sucrose, pH 7.4, at 4 °C. Lysate was layered onto a solution of 27% (wt/vol) sucrose in Beckman SW-27.1 tubes, and centrifuged at $80{,}000 \times g$ for 4 hr.

The plasma membrane fraction was recovered slightly below the sucrose-buffer interface, suspended in 3.3 × its volume of buffer, pelleted at $96{,}500 \times g$ for 45 min in a Beckman 50-Ti rotor and resuspended in lysate buffer. This fraction was highly enriched in the plasma membrane marker enzymes Na^+,K^+-ATPase (3.9-fold over that in lysate) and acid phosphatase (3.1-fold), but depleted in the granular marker enzyme beta-glucuronidase (0.7-fold) [for assays, *see* Ref. 1]. Electronmicrographs of this fraction taken with a Hitachi HU11E indicated membrane vesicles, ranging in diameter from approximately 70 to 200 nm; many vesicles were double-layered. Our fraction appears to be highly enriched in platelet plasma membrane fragments, in good agreement with Barber and Jamieson [1].

Temperature-Dependent Studies on the Activity of Platelet Membrane Acid Phosphatase

On the same day that blood was drawn from normal donors, platelet lysates or purified platelet plasma membranes were used to examine acid phosphatase activity. For all temperatures tested, linear time courses were obtained for acid phosphatase activity [25]; initial rates were calculated, and the final pH was kept constant at 4.8. Arrhenius plot data were handled by a computer-fitting process which utilizes least-squares minimalization to assign break points and to determine activation energies [19].

Spin-Labeling of Human Platelet Plasma Membranes and Rat Liver Plasma Membranes

Methods for ESR studies were essentially as described previously in some detail [5, 13, 14]. For spin-label studies, platelet membranes were suspended in 50 mM Tris-HCl, 8% (wt/vol) sucrose, pH 7.4, at 3.8 mg protein/ml, while liver membranes were suspended in 50 mM triethanolamine-HCl, 8% (wt/vol) sucrose, pH 7.6, at 4 mg protein/ml. Membranes were used fresh or after storage at −70 °C; no spectral differences were noted between fresh and frozen membranes. Incorporation of I(12,3) and spectral recording were as set out in Gordon et al. [13].

Evaluation of the Flexibility of the Membrane-Incorporated I(12,3) Probe

The following order parameter expressions [11] may be used to evaluate the flexibility of the membrane-incorporated fatty acid spin probe:

$$S(T_{\parallel}) = 1/2\left[\frac{3(T_{\parallel} - T_{xx})}{(T_{zz} - T_{xx})} - 1\right], \tag{1}$$

$$S(T_{\perp}) = 1/2\left[\frac{3[(T_{zz} + T_{xx}) - 2T_{\perp}]}{(T_{zz} - T_{xx})} - 1\right], \tag{2}$$

$$S = \frac{(T_{\parallel} - T_{\perp})(a_N)}{(T_{zz} - T_{xx})(a'_N)}. \tag{3}$$

Here, $T_{\parallel}$ and $T_{\perp}$ are the hyperfine splitting elements parallel and perpendicular to z', the symmetry axis of the effective Hamiltonian (**H′**), and T_{xx} and T_{zz} are the hyperfine splitting elements of the static interaction tensor (**T**) parallel to the static Hamiltonian (**H**) principal nuclear hyperfine axes x and z. The x-axis is parallel to the N–O bond direction, and the z-axis is parallel to the nitrogen $2p\pi$ orbital. Elements of **T** were earlier determined by incorporating nitroxide derivatives into host crystals: $(T_{xx}, T_{zz}) = (6.1, 32.4)$ G [11]. A'_N and a_N are the isotropic hyperfine coupling constants for probe in membrane and crystal states [i.e., $a'_N = 1/3(T_{\parallel} + 2T_{\perp})$ and $a_N = 1/3(T_{zz} + 2T_{xx})$].

The order parameters S, $S(T_{\parallel})$ and $S(T_{\perp})$ are sensitive to membrane fluidity (or, more accurately, the flexibility of the membrane-incorporated probe). S, $S(T_{\parallel})$ and $S(T_{\perp})$ may each assume values between 0 and 1, with the extreme limits indicating that the probe samples fluid and immobilized environments. The order parameter S, which requires both hyperfine splittings, corrects for small polarity differences between the membrane and reference crystal. Although $S(T_{\parallel})$ and $S(T_{\perp})$ do not include polarity corrections, these expressions have been found to be useful fluidity approximations [11]. However, the above theoretical treatment is valid only if electron-electron exchange and dipole-dipole interactions make negligible contributions to **H′** [5, 28].

Estimation of Probe-Probe Interactions in I(12,3)-Labeled Biological Membranes

Two measures of probe-probe interaction are employed here [5, 13, 28]. The first index involves the determination of the ΔH of the mid-field linewidth (*see* Fig. 3 of Sauerheber et al. [29]),

$$\Delta H = \Delta H_o + \Delta H_{dip} + \Delta H_{ex} \tag{4}$$

where ΔH_o is the linewidth without interactions, ΔH_{dip} is the line-broadening caused by magnetic dipolar interactions and ΔH_{ex} is contributed by spin-spin exchange [5]. Enhanced probe-probe interactions lead to an increase in ΔH. The second measure is based on the observation that $T_{\perp}$, but not $T_{\parallel}$, broadens with increasing probe concentration in various membranes [5,

28]. Consequently, for those probe concentrations where the percent change in $S(T_{\|})$, $\Delta S(T_{\|})$, is zero, decreases in $S(T_{\perp})$ with increasing probe concentration reflect enhanced I(12,3) clustering.

Results and Discussion

The Effects of I(12,3) Concentration on the Order Parameters of Human Platelet Plasma Membranes

ESR spectra of platelet membranes labeled with a low I(12,3) concentration indicate that the incorporated probe undergoes rapid anisotropic motion about its long molecular axis at physiologic temperatures. These spectra and those at high probe loading are comparable to spectra obtained from I(12,3)-labeled intact platelets (Figs. 1 and 6 of Sauerheber et al. [29]). Increasing the probe/mg membrane protein ratio decreased the high-field peak of the inner hyperfine doublet, displaced downward the high-field baseline and upward the low-field baseline, increased $2T_{\perp}$ and ΔH, and left $2T_{\|}$ unchanged.

As the probe concentration in platelet membranes was increased over a wide range at 37 °C, S and $S(T_{\perp})$ decreased substantially, while $S(T_{\|})$ remained essentially constant (Fig. 1*A*). These order parameter effects are most likely attributed to enhanced probe-probe interactions, and are not due to membrane fluidization. The broadening of $T_{\perp}$ [and decrease in $S(T_{\perp})$] was closely correlated with increases in ΔH (e.g., Fig. 6 of Ref. [29]); previous investigations have shown that radical interactions broaden the ΔH of labeled model and biological membranes (for reviews, *see* Refs. [5, 28]). Decreases in S and $S(T_{\perp})$ were also associated with such characteristic exchange-broadened effects as the decrease in the high-field peak height of the inner hyperfine doublet and the downward displacement of the high-field baseline (*see* Fig. 2 in Gordon et al. [13]). The observation that $T_{\|}$ [and $S(T_{\|})$] is essentially unaltered for platelet membranes (Fig. 1) indicates that the "apparent" increase in fluidity with probe concentration, denoted by reductions in S and $S(T_{\perp})$, is not the result of probe-mediated membrane perturbations; any fluidization that permits more probe flexibility requires that $T_{\|}$ decrease commensurately with increases in $2T_{\perp}$ and that ΔH narrows. Similar I(m, n) concentration effects on order parameters have been observed in many other biological membranes, including intact platelets [5]. For probe ranges where $\Delta S(T_{\|})$ is zero, $\Delta S(T_{\perp})$ provides us with an empirical parameter sensitive to probe-probe interactions.

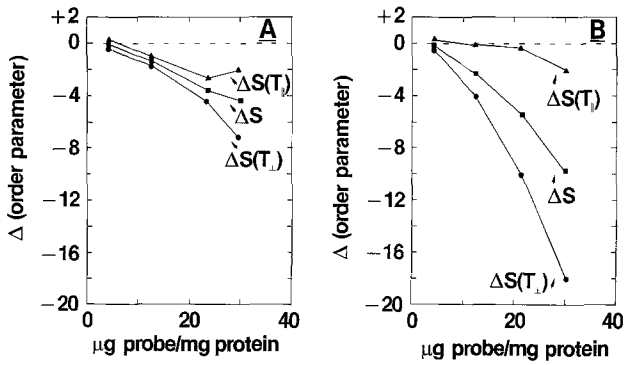

Fig. 1. Effects of increasing I(12,3) concentration on order parameters of human platelet plasma membranes at 37° and 25 °C. (*A*) ΔS, $\Delta S(T_{\|})$ and $\Delta S(T_{\perp})$ are percent changes in order parameters from values measured at 4 μg probe/mg protein at 37 °C; control values of S, $S(T_{\|})$ and $S(T_{\perp})$ are 0.620, 0.665 and 0.585. (*B*) ΔS, $\Delta S(T_{\|})$ and $\Delta S(T_{\perp})$ are percent changes in order parameters from values measured at 4 μg probe/mg protein at 25 °C; control values of S, $S(T_{\|})$ and $S(T_{\perp})$ are 0.678, 0.760 and 0.625

Probe-probe interactions are apparently negligible for I(12,3) concentrations less than approximately 12 μg probe/mg protein at 37 °C (Fig. 1*A*). Consequently, the S, $S(T_{\|})$ and $S(T_{\perp})$ control values reflect 'intrinsic' or 'magnetically dilute' order parameters that are independent of radical interaction effects [28].

I(12,3) titrations were also conducted on platelet membranes at 25 °C. Qualitatively similar spectral alterations were observed with increasing probe concentration at 25° or 37 °C, although the magnitude of radical interaction effects at comparable probe/membrane protein ratios was greater at the lower temperature. Fig. 1*B* shows that S and $S(T_{\perp})$ decreased while $S(T_{\|})$ remained constant with increasing probe concentration. However, the percent decline in S and $S(T_{\perp})$ was much greater at 25 °C than at 37 °C over the same range of probe/mg protein ratios. Extrapolation of the S and $S(T_{\perp})$ curves in Fig. 1*B* to 'zero' probe concentration indicates that the order parameters in the legend are underestimated by no more than 1 and 2%, respectively. After incorporation of these minor corrections, lowering the temperature by 12 °C increases S, $S(T_{\|})$ and $S(T_{\perp})$ by 9.9, 13.3 and 8.6%.

It is unlikely that the probe concentration dependence of order parameters (Fig. 1*A*) is the result of increased dipole interactions, but rather is due to enhanced spin-exchange arising from I(12,3) clustering. This is because the probe exhibits rapid anisotropic motion at 37 °C and dipole-dipole interactions are relatively long range, tending to be averaged out by rapid diffusion and/or tumbling, while exchange interactions require that labels be in van der Waal's contact and decrease

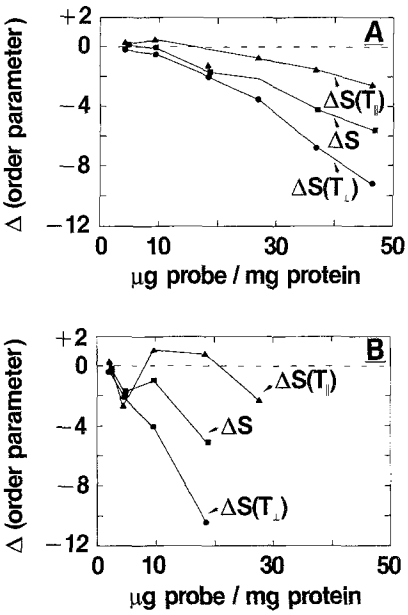

Fig. 2. Effects of increasing I(12,3) concentration on order parameters of native and cholesterol-enriched rat liver plasma membranes at 36 °C. (*A*) ΔS, $\Delta S(T_{\parallel})$ and $\Delta S(T_{\perp})$ are percent changes in native membrane (C/P = 0.71) order parameters from values measured at 4 μg probe/mg protein; control values of S, $S(T_{\parallel})$ and $S(T_{\perp})$ are 0.558, 0.585 and 0.538. (*B*) ΔS, $\Delta S(T_{\parallel})$ and $\Delta S(T_{\perp})$ are percent changes in cholesterol-enriched membrane (C/P = 0.85) order parameters from values measured at 2 μg probe/mg protein; control values of S, $S(T_{\parallel})$ and $S(T_{\perp})$ are 0.620, 0.675 and 0.577

rapidly with distance. In platelet membranes, probe-probe interaction effects are greater at 25 °C (Fig. 1 *B*) than at 37 °C (Fig. 1 *A*). This is most likely attributed to increased spin-exchange interactions due to greater I(12,3) clustering at 25 °C. The alternate interpretation that this is due to increased dipole-dipole interactions for uniformly distributed probe is improbable for several reasons. First, I(12,3) undergoes rapid, anisotropic motion about its long molecular axis at both 25° and 37 °C, and this would tend to average out dipolar broadening contributions. A second point is based on the fact that spin-exchange interactions for homogeneously distributed probe should decrease upon temperature reduction, since cooling would be expected to lower the lateral diffusion of the spin probe in the bilayer. Consequently, temperature reductions for uniformly distributed probe would be predicted to exert opposing actions on radical interaction effects: spin-exchange would decrease while dipole-dipole would increase. Without probe clustering, the only circumstance under which radical interactions would increase with decreasing temperature would be if dipolar broadening contributions were much greater than those of spin exchange at physiologic temperatures. Since dipolar broadening effects are likely to be small at high temperatures due to rapid I(12,3) motions, we accordingly reject the uniform distribution model. Instead, we believe that the enhanced probe-probe interactions in platelet membranes at 25 °C are due to I(12,3) segregation, and that this probe clustering is mediated by a lateral redistribution of native lipid components.

The Effects of I(12,3) Concentration on the Order Parameters of Native and Cholesterol-Enriched Rat Liver Plasma Membranes

The functional dependence of order parameters on the I(12,3) concentration was determined for native (Fig. 2 *A*) and cholesterol-enriched (Fig. 2 *B*) rat liver plasma membranes at 36 °C. $S(T_{\parallel})$ was relatively independent of the probe concentrations used here. However, S and $S(T_{\perp})$ decreased substantially if the I(12,3) concentration exceeded 18 or 5 μg/mg protein in native and cholesterol-enriched membranes, respectively; the decrease in $S(T_{\perp})$ was greater than the corresponding decrease in S for each membrane. These order parameter changes are similar to those observed earlier with human platelet plasma membranes (Fig. 1) and native rat liver plasma membranes [13, 28]. For experimentally determined low probe concentrations, elevating the C/P ratio of native liver plasma membranes from 0.71 to 0.85 increased S, $S(T_{\parallel})$ and $S(T_{\perp})$ by 10.5, 14.3 and 7.0%, respectively.

Cholesterol loading of rat liver plasma membranes achieves alterations in probe flexibility and clustering at 36 °C analogous to those induced in platelet membranes by temperature reduction. 'Magnetically dilute' order parameters derived from Fig. 2 show that increasing the C/P ratio markedly decreases the fluidity, in agreement with results of an earlier study [33]. This is consistent with previous investigations showing that cholesterol exerts an ordering and condensing effect on model phospholipid bilayers above their melting point [24]. Cholesterol loading also promotes I(12,3) clustering, as indicated in Fig. 2 by the increased radical interactions noted at lower probe/protein ratios. One explanation of these latter actions is that cholesterol-rich and -poor lipid domains are formed, such that I(12,3) tends to be excluded from cholesterol-rich domains. It is well known from model studies that cholesterol interacts preferentially with specific phospholipids [7, 8], and in biological membranes this may create domains of differing fluidity [24]. As spin probes have been reported to distribute inhomogeneously

in mixed model membranes [4], I(12,3) may partition nonuniformly among newly created cholesterol-rich and -poor domains in cholesterol-loaded rat liver plasma membranes. Certainly, it would not be surprising for I(12,3) to be selectively excluded from cholesterol-rich lipid domains. Although the precise orientation of cholesterol has been the subject of some controversy, this molecule is now believed to insert rather deeply into the bilayer. In this way, its beta-hydroxyl group participates in hydrogen bonding with the carbonyl oxygen linking the phospholipid fatty acyl chain with its glycerol backbone, and the rigid nucleus interacts with adjacent fatty acyl chains [20]. I(12,3), with its bulky oxazolidine reporter group projecting from the 4th carbon from the carboxyl terminus, would not be expected to readily partition into such cholesterol-rich domains, as it would have to disrupt closely interacting cholesterol/phospholipid adducts. Thus, enrichment of liver membranes with cholesterol may form cholesterol-rich and -poor domains at 36 °C, and this tends to sequester I(12,3) in cholesterol-poor domains and enhances radical interactions by raising the 'effective' probe/lipid ratio. Since temperature reductions of platelet membranes similarly decrease probe flexibility and enhance probe clustering (Fig. 1), we suggest that cholesterol-rich domains are also created in this membrane at low temperatures.

The Thermotropic Lipid Phase Separation in I(12,3)-Labeled Native Rat Liver Plasma Membranes

Arrhenius-type plots of S, $S(T_\parallel)$ and $S(T_\perp)$ were obtained for native liver membranes labeled with a low probe concentration. Figure 3*A* shows the presence of characteristic 'breaks' or 'discontinuities' at 19° and 28 °C in each order parameter curve; breaks at these temperatures were also noted in Arrhenius plots of order parameters. Increasing the μg probe/mg protein ratio to 22 dramatically alters Arrhenius-type plots of the order parameters (Fig. 3*B*). The 'break' at 28 °C is abolished in each curve, while the break at 19 °C in the $S(T_\parallel)$ plot is less discernible. Probe loading decreases the S and $S(T_\perp)$ values in Fig. 3*B* with respect to those in Fig. 3*A*, and increases the divergence of the S and $S(T_\perp)$ curves vis a vis that of $S(T_\parallel)$.[1]

[1] S and $S(T_\perp)$ could not be determined for temperatures less than 10° and 20 °C in Fig. 3*A* and *B*, respectively, due to the poorly resolved inner hyperfine doublet, $2T_\perp$ (e.g., Fig. 2*E* in Ref. 13). For similar reasons, S and $S(T_\perp)$ were not calculated at low temperatures in Figs. 5 and 7.

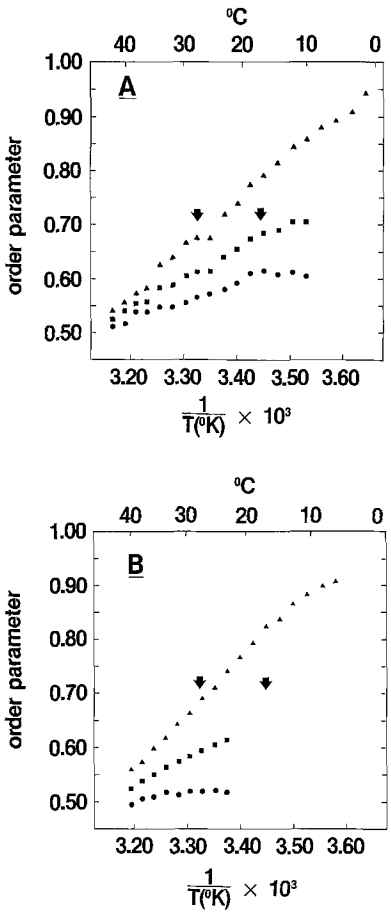

Fig. 3. Temperature dependence of S [■], $S(T_\parallel)$ [▲] and $S(T_\perp)$ [●], calculated from spectra of I(12,3)-labeled native rat liver plasma membranes (C/P = 0.71). (*A*) Membranes labeled with 2.7 μg probe/mg protein. Arrows indicate apparent 'breaks' at 28° and 19 °C. (*B*) Membranes labeled with 22 μg probe/mg protein. The low and high temperature breaks are not readily apparent in (*B*) (*see* Results and Discussion)

Difference native liver plasma membrane order parameter *versus* $1/T$(°K) plots were calculated as the percent difference between values obtained at 'high' and 'low' probe concentrations for each temperature. Figure 4 indicates that $\Delta S(T_\perp)$ and ΔS become increasingly more negative for temperatures below 28 °C, while $\Delta S(T_\parallel)$ did not significantly vary from zero. The relative invariance of $S(T_\parallel)$ noted in Fig. 4 suggests that, for 'low' and 'high' probe concentrations, ESR spectra reflect only those I(12,3) which sample lipid domains sharing the same fluidity and polarity. Since it is reasonable to assume that the flexibility and polarity contributions to 'low' and 'high' range $S(T_\parallel)$ will be equal at a given temperature [5], $\Delta S(T_\perp)$ (or, alternatively, $\Delta T_\perp$) is here an empirical parameter reflecting only radical interactions. It should be recalled that $S(T_\perp)$ decreased as the I(12,3) concentration increased in liver membranes at 36 °C,

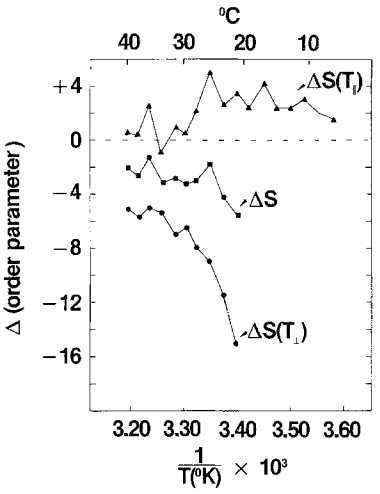

Fig. 4. Temperature dependence of ΔS [■], $\Delta S(T_{\parallel})$ [▲] and $\Delta S(T_{\perp})$ [●] for native rat liver plasma membranes (C/P = 0.71). Δ (order parameter) was calculated at a given temperature as the percent difference between values measured at high (μg I(12,3)/mg protein of Fig. 3*B*) and low (μg I(12,3)/mg protein of Fig. 3*A*) probe concentrations

while $S(T_{\parallel})$ remained unchanged. The observation that $\Delta S(T_{\perp})$ in Fig. 4 becomes more negative for temperatures below 28° therefore suggests that lowering the temperature also promotes probe-probe interactions in native liver membranes.

These experiments indicate a thermotropic (temperature-dependent) lipid phase separation in native rat liver plasma membranes, in agreement with previous studies employing various techniques (for reviews, *see* Refs. [17, 26]). Using low probe concentrations, Arrhenius-type plots of the order parameters of liver membranes demonstrated breaks at 19° and 28 °C (Fig. 3*A*), suggesting that a lipid phase separation between these temperatures perturbs I(12,3) flexibility. For reasons discussed previously in some detail [13], we proposed that solid (**S**) and liquid (**L**) lipid domains coexist in rat liver plasma membranes at temperatures less than 19 °C. The 19 °C break in Fig. 3*A* would then correspond to **S** and **L** being dispersed into "quasicrystalline" clusters (**QCC**) and **L**.[2] Here, **QCC** are defined as having a packing density and fluidity between that of **S** and **L**. The percentage of **QCC** will decrease with increases in temperature above 19 °C until the 28 °C transition is reached and the remaining **QCC** are converted into **L**. Consequently, enhanced I(12,3) clustering detected in Arrhenius-type plots of difference order parameters of native membranes for temperatures less than 28 °C (Fig. 4) suggests that the formation of probe-excluding **QCC** tends to segregate I(12,3) in **L** domains. As we are now able to mimic this probe clustering effect isothermally at 36 °C, simply by raising the C/P ratio (Fig. 2), then it would not be unreasonable to propose that the **QCC** in native membranes below 28 °C are cholesterol-rich domains. This would agree with the marked depression of the thermotropic lipid phase separation of native liver membranes achieved by agents (i.e., benzyl alcohol and phenobarbital) known to disrupt cholesterol-rich domains in model membranes [14, 16]. Also consistent with our hypothesis is the finding that the thermal transition observed in these membranes is broad and of low enthalpy; the relatively low cooperativity of the transition may reflect the melting of cholesterol-rich domains [26].

[2] In rat liver plasma membranes, **S** is close-packed, gel lipid yielding an electron diffraction band at 4.12 Å, **L** is liquid-crystalline lipid with a diffraction band at 4.6 Å [21], while **QCC** represents 'quasi-crystalline' lipid with diffraction bands overlapping that of **L**. I(12,3) is excluded from both **S** and **QCC** and tends to reside in **L** [13].

The Thermotropic Lipid Phase Separation in Cholesterol-Enriched Rat Liver Plasma Membranes

An Arrhenius-type plot of the $S(T_{\parallel})$ of cholesterol-enriched rat liver plasma membranes (C/P = 0.85), labeled with a low probe concentration, indicates 'breaks' at 37° and 18 °C (Fig. 5*A*). This suggests that cholesterol-loading raises the high-temperature onset of the lipid phase separation from 28° to approximately 37 °C, without significantly altering the onset at 18° to 19 °C. It should, however, be noted that these 'breaks' are less noticeable in Arrhenius-type plots of S and $S(T_{\perp})$ (Fig. 5*A*). Elevated probe concentrations markedly perturb the form of Arrhenius-type plots of order parameters (Fig. 5*B*). Although probe loading blunts the sensitivity of $S(T_{\parallel})$ to 'breaks' at 37° and 18 °C, $S(T_{\parallel})$ derived from cholesterol-enriched membranes labeled with either low (Fig. 5*A*) or high (Fig. 5*B*) probe concentrations were in good agreement. Contrarily, high-range S and $S(T_{\perp})$ values were much below those noted with membranes labeled with a low probe concentration (Fig. 5*A, B*). Cholesterol-enrichment also profoundly modulate the form of Arrhenius-type plots of Δ (order parameters); the high temperature onset at which I(12,3) becomes clustered is raised from 28° to 37° C, since $S(T_{\perp})$ now declines at the higher temperature, while $S(T_{\parallel})$ remains unchanged (Fig. 6*A*).

These spin-label studies provide evidence that cholesterol enrichment perturbs order parameters in a manner consistent with cholesterol-rich and -poor lipid domains being initially present in native

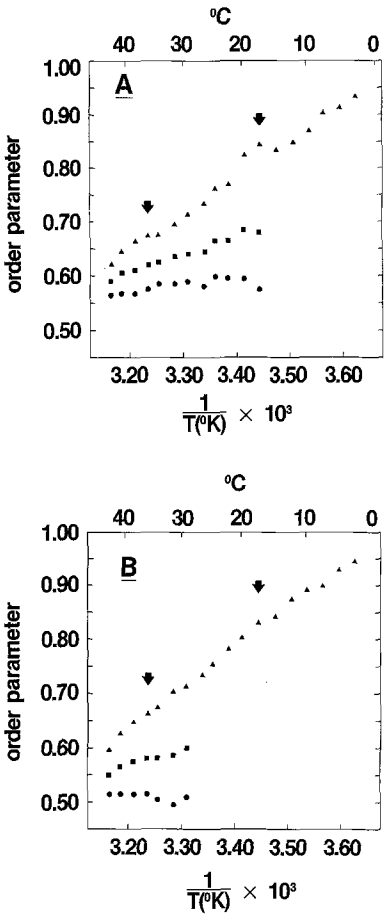

Fig. 5. Temperature dependence of S [■], $S(T_{\|})$ [▲] and $S(T_{\perp})$ [●], calculated from spectra of I(12,3)-labeled, cholesterol-enriched rat liver plasma membranes (C/P = 0.85). (*A*) Membranes labeled with 4 μg probe/mg protein. Arrows indicate apparent break temperatures at 37° and 18 °C. (*B*) Membranes labeled with 19 μg probe/mg protein. Low and high temperature breaks at 19° and 37 °C are not readily apparent in (*B*) (*see* Results and Discussion)

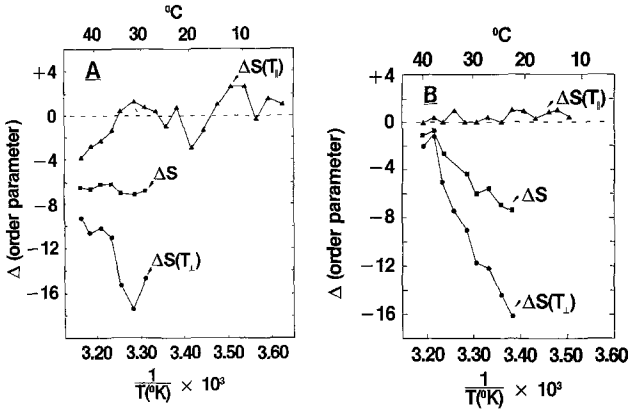

Fig. 6. Temperature dependence of ΔS [■], $\Delta S(T_{\|})$ [▲] and $\Delta S(T_{\perp})$ [●] for cholesterol-enriched rat liver plasma membranes (C/P = 0.85) and human platelet plasma membranes. (*A*) Δ (order parameter) was calculated from cholesterol-enriched liver membranes at a given temperature as the percent difference between values measured at high (μg I(12,3)/mg protein of Fig. 5*B*) and low (μg I(12,3)/mg protein of Fig. 5*A*) probe concentrations. (*B*) Δ (order parameter) was calculated from platelet membranes at a given temperature as the percent difference between values measured at high (μg I(12,3)/mg protein of Fig. 7*B*) and low (μg I(12,3)/mg protein ratio of Fig. 7*A*) probe concentrations

liver plasma membranes. For low I(12,3) concentrations, Arrhenius-type plots of $S(T_{\|})$ indicated that cholesterol loading abolished the 28° C break and elevated the high temperature onset of the phase separation to 37° C, while leaving the break at 18° C unaffected (Fig. 5*A*). This agrees with previous Arrhenius-type plots of $S(T_{\|})$ derived from cholesterol-enriched rat liver plasma membranes (C/P = 0.96), except that the high temperature break was not identified in the earlier study due to the use of a restricted temperature range [33]. Arrhenius-type plots of Δ (order parameters) (Figs. 4 and 6*A*) confirm that cholesterol loading raises the onset temperature at which I(12,3) clusters from 28° C in native membranes to 37 to 38° C. The simplest explanation is that cholesterol incorporation promotes the formation of **QCC** at higher temperatures. **QCC** observed in high-cholesterol membranes at temperatures greater than 28° C are similar to those in native membranes at temperatures less than 28° C, since both facilitate I(12,3) clustering. Consequently, certain of those phospholipid species participating in the **QCC** of native membranes are also likely, on cholesterol loading, to be recruited into **QCC** at temperatures higher than 28° C. Our finding that the low temperature discontinuity remains at 19° C in the manipulated membranes suggests that the 19° C break, which we attributed to the aggregation of **QCC** to **S** [13, 14], is undisturbed by cholesterol loading.

The Thermotropic Lipid Phase Separation in I(12,3)-Labeled Human Platelet Plasma Membranes

For platelet membranes labeled with a 'low' probe concentration, Arrhenius-type plots of $S(T_{\|})$ vary as a smooth function of temperature (Fig. 7*A*). Contrarily, plots of S and $S(T_{\perp})$ show significant curvature, with 'breaks' at approximately 22° C. Figure 7*A* also indicates that the slopes of the order parameter *vs.* $1/T$(°K) curves become steeper in the following order: $S(T_{\perp}) < S < S(T_{\|})$. Using a 'high' probe concentration (Fig. 7*B*), there is no longer any indication of curvature in Arrhenius-type plots of either S or $S(T_{\perp})$. Although S and $S(T_{\|})$ decrease with increasing temperature in Fig. 7*B*, $S(T_{\perp})$ was found to increase with increas-

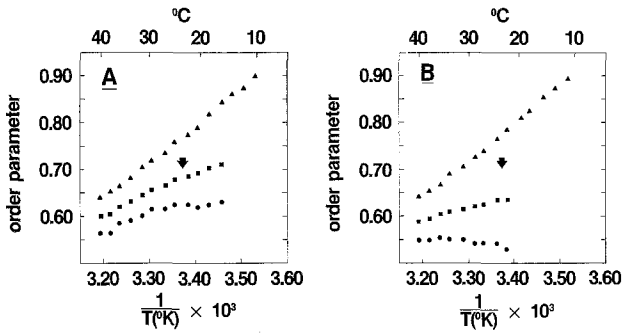

Fig. 7. Temperature dependence of S [■], $S(T_{\|})$ [▲] and $S(T_{\perp})$ [●], calculated from spectra of I(12,3)-labeled human platelet plasma membranes. (*A*) Membranes labeled with 12 μg probe/mg protein. The arrow indicates an apparent break at 22 °C. (*B*) Membranes labeled with 30 μg probe/mg protein. The low temperature break at 22 °C is not apparent in (*B*) (*see* Results and Discussion)

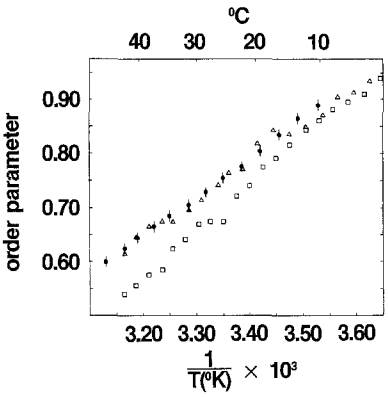

Fig. 8. Temperature dependence of $S(T_{\|})$ values of I(12,3)-labeled human platelet plasma membranes [●], native rat liver plasma membranes (C/P = 0.71) [□], and cholesterol-enriched rat liver plasma membranes (C/P = 0.85) [△]. Platelet membranes were labeled with 12 μg I(12,3)/mg protein; results are means ± 1 SD for three preparations. Native and cholesterol-enriched liver membranes were labeled with 2.7 and 4 μg I(12,3)/mg protein

ing temperature. The anomalous behavior of the high range $S(T_{\perp})$ *vs.* $1/T(°K)$ is likely due to elevated radical interactions manifest in platelet membranes at low temperatures. We note that Arrhenius-type plots of $S(T_{\|})$ obtained from platelet membranes labeled with either a low or high I(12,3) concentration were in excellent agreement (Fig. 7). However, high range S and $S(T_{\perp})$ in Fig. 7*B* were considerably less than the corresponding values measured using the low probe/mg protein ratio of Fig. 7*A* for each temperature in the range 22° to 40 °C. Arrhenius-type plots of Δ (order parameters) for platelet membranes (Fig. 6*B*) indicate that $\Delta S(T_{\perp})$ and ΔS become increasingly more negative for temperatures below 37 °C, while $\Delta S(T_{\|})$ did not vary from zero. This indicates that lowering the temperature below 37 °C promotes radical interactions and probe clustering in human platelet plasma membranes.

The above spin-label studies demonstrate the existence of a thermotropic lipid phase separation in human platelet plasma membranes between 37° and 22 °C. The onset at 37 °C was principally identified from Δ (order parameter) plots (Fig. 6*B*) as the temperature at which I(12,3) begins to segregate. Although a low temperature 'break' at approximately 22 °C was tentatively assigned from Arrhenius-type plots of S and $S(T_{\perp})$ for plasma membranes labeled with a low I(12,3) concentration, there was no indication of a 37 °C break in such plots (Fig. 7). In I(12,3)-labeled intact platelets [29], we showed that I(12,3) primarily samples the surface membrane; similar to results obtained with spin-labeled platelet plasma membranes, no breaks were identified in Arrhenius-type of $S(T_{\|})$ for whole platelets. Arrhenius-type plots of Δ (order parameters) are apparently more reliable in monitoring the high temperature onset of the lipid phase separation than are Arrhenius-type plots of the order parameters of purified platelet plasma membranes.

Temperature-Dependence of Order Parameters Derived from Human Platelet Plasma Membranes, Native and Cholesterol-Enriched Rat Liver Plasma Membranes

Figure 8 shows temperature effects on the $S(T_{\|})$ of I(12,3)-labeled human platelet plasma membranes, native and cholesterol-enriched rat liver plasma membranes. The $S(T_{\|})$ values of native liver membranes (C/P = 0.71) were much less than cholesterol-enriched liver membranes (C/P = 0.85) for temperatures in the range 17° to 42 °C, with the largest difference in $S(T_{\|})$ occurring at the highest temperature. However, $S(T_{\|})$ of native and cholesterol-enriched rat liver plasma membranes were little different for temperatures less than approximately 17 °C. Particularly striking is the overlap of the $S(T_{\|})$ curves for platelet plasma membranes and cholesterol-enriched liver plasma membranes over the range 10° to 42 °C.

Comparison of the thermodependent $S(T_{\|})$ values of native and cholesterol-enriched rat liver plasma membranes verifies that cholesterol loading achieves effects in addition to **QCC** formation at high temperatures (Fig. 8). On raising the tempera-

ture above 18 °C, I(12,3) flexibility in high-cholesterol membranes became increasingly less with respect to native membranes up to the highest temperature tested (i.e., 42 °C). Such actions are in accord with the ability of cholesterol, when added to model lipids at temperatures above their bulk melting point, to increase the order of lipid fatty acyl chains [24]. Spin probe clustering decreases with increasing temperature over the same temperature range that cholesterol-enriched membranes become more rigid, vis a vis native membranes (Figs. 6*A* and 8). We attribute this inverse relationship to the disruption of cholesterol-rich **QCC** which first releases sterol into the **L** domains sampled by probe, and then reduces I(12,3) segmental flexibility. Our finding that $S(T_{\|})$ values of native and high-cholesterol membranes are similar for temperatures less than 18 °C may be explained if the additional cholesterol/phospholipid adducts formed in high-cholesterol membranes remain associated at lower temperatures. Although the size of the **L** domains sampled by I(12,3) would be smaller in cholesterol-enriched membranes, the $S(T_{\|})$ reported by I(12,3) would be the same in both membranes because the fluidity of each **L** is similar.

There are several striking similarities between the spin-label properties of human platelet plasma membranes (C/P = 0.50 from Shattil and Cooper [30]) and cholesterol-enriched rat liver plasma membranes (C/P = 0.85). First, the $S(T_{\|})$ values for these two membranes lie within experimental error over a wide temperature range (Fig. 8). Second, both platelet membranes and cholesterol-enriched liver membranes identically segregate I(12,3) for temperatures less than 37 °C (Fig. 6*A*, *B*). Thus, cholesterol enrichment of rat liver plasma membranes achieves an 'artificial' system which is degenerate when compared to human platelet plasma membranes, with respect to temperature-dependent probe clustering and mobility. Since cholesterol-rich **QCC** form in high-cholesterol rat liver plasma membranes, it is tempting to speculate that similar cholesterol-rich **QCC** occur in human platelet plasma membranes for temperatures less than 37 °C. According to this model, the low temperature break at 22 °C, tentatively assigned from Fig. 7*A*, would reflect **QCC**→**S**. Of course, additional spin-label experiments on cholesterol-manipulated platelet plasma membranes will be required before this hypothesis can be verified.

Our finding that a thermotropic lipid phase separation exists in human platelet plasma membranes for temperatures less than 37 °C appears to contradict results of previous probe studies. In platelets labeled with the fluorescent probe diphenylhexatriene (DPH), Arrhenius plots of DPH rotational mobility showed only straight lines [3, 30, 31]; these results indicate that DPH does not "sense" any platelet membrane phase separation or transition. Perhaps the formation of **QCC** domains is not detected by DPH due to selective partitioning of the probe. Both I(*m*, *n*) [4] and various fluorescence probes [2] have been reported in binary phase, model lipid systems to preferentially distribute into the more fluid domain. As long as either I(12,3) or DPH remain in **L**, the gradual accretion of **QCC** might only minimally affect Arrhenius plots of probe mobility. This would explain why Arrhenius-type plots of order parameters (Fig. 7) and DPH rotational mobility [3, 30, 31] are insensitive to the high temperature onset of the lipid phase separation in platelet plasma membranes. Even in Arrhenius-type plots of order parameters of native and cholesterol-rich rat liver plasma membranes using low probe concentrations (Figs. 3*A* and 5*A*), the high temperature breaks are not particularly dramatic; this would be consistent with the formation of **QCC** exerting only 'second-order' effects on probe mobility. The rather subtle actions of **QCC** and **S** on I(12,3) flexibility might explain how $S(T_{\|})$ values of human platelet plasma membranes and cholesterol-rich rat liver plasma membranes can be in good agreement in Fig. 8, yet only high-cholesterol liver membrane Arrhenius-type plots of $S(T_{\|})$ exhibit characteristic 'breaks' (Fig. 5*A*). Contrarily, Arrhenius-type plots of A (order parameters) are exquisitely sensitive to the ratio of **QCC** to **L**, as increases in this ratio would greatly enhance probe clustering and radical interactions.

Arrhenius Plots of Human Platelet Acid Phosphatase Activity

The temperature-dependent activity of acid phosphatase, an enzyme marker of plasma membranes, was similar when examined using either platelet lysates or purified platelet plasma membranes (Fig. 9). In plasma membranes, Arrhenius plots of activity over the range 25° to 45 °C were biphasic with a break at 36.2° ± 1.9 °C (SD, $n = 3$ determinations); heats of activation above and below the break point were 21 ± 9 and 58.5 ± 6.4 kJ mol^{-1}, respectively. For platelet lysates, Arrhenius plots indicated a break at 35.6° ± 1.7 °C (SD, $n = 5$ determinations); heats of activation above and below the break temperature were 25.0 ± 8.1 and 59.3 ± 6.4 kJ mol^{-1}, respectively. The primary difference between these plots is that the specific ac-

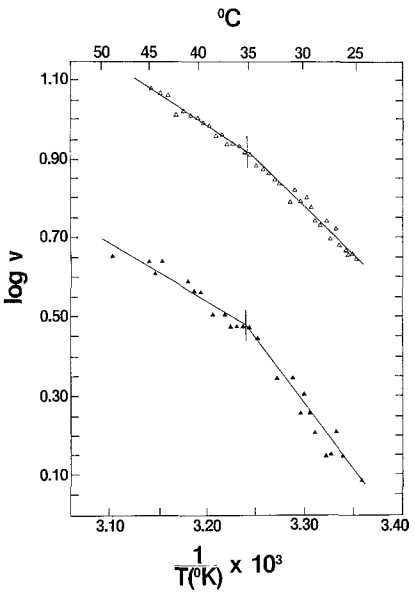

Fig. 9. Arrhenius plots of acid phosphatase activity in platelet lysates [▲] and purified platelet plasma membranes [△]. The activity (v) is expressed as μmol product mg protein^{-1} hr^{-1}. Vertical hash marks indicate the 'break' temperature at 35 °C

tivity of acid phosphatase in purified membranes is three- to fourfold greater than in platelet lysates.

It is likely that the high temperature onset of the lipid phase separation in platelet plasma membranes is responsible for the break at 36 °C noted in Arrhenius plots of acid phosphatase activity. Such an assignment would be in accord with much evidence indicating that lipid phase separations occurring in other biological membranes can influence the activity of penetrant enzymes [27]. In native rat liver plasma membranes, Arrhenius plots of activity for a variety of integral enzymes show 'breaks' at 28 °C and sharply elevated activation energies below the break point [17]. These effects may be directly or indirectly due to the high temperature onset of the lipid phase separation in native liver membranes, which here has been attributed to the formation of cholesterol-rich **QCC** in a cholesterol-poor **L** matrix. For example, the increase in **QCC** as the temperature is lowered below 28 °C may segregate proteins in a relatively small **L** phase, perhaps inhibiting enzyme activity by promoting protein-protein interactions. Alternatively, the formation of **QCC** may restrict the availability to the enzyme of phospholipids that are critical for maintaining maximal activity. As a similar thermotropic lipid phase separation occurs in platelet plasma membranes, it would not be unreasonable to hypothesize that the break at 36 °C in the Arrhenius plot of platelet acid phosphatase activity is due to the formation of cholesterol-rich **QCC** in a cholesterol-poor **L** matrix. It is also tempting to speculate that other platelet surface phenomena will be influenced by this thermotropic lipid phase separation. In a recent study of platelet aggregation kinetics measured by quenched flow techniques, Gear [10] reported a narrow temperature range (35° to 40 °C) over which platelet aggregation velocity was optimal; aggregation became inhibited for temperatures outside this range. Clearly, future experiments elucidating possible relationships between aggregation and the thermotropic lipid phase separation of platelet plasma membranes will be of much interest.

We thank Drs. Cyril Curtain and Adrian Gear for commenting on the manuscript. This work was supported by a Medical Research Council project grant, NATO Research Grant (RG218.80) and Wellcome Trust Travel Fellowship (MDH); a Science Research Council Studentship (ADW); grants-in-aid from the American Diabetes Association, Southern California Affiliate, Inc., the Kroc Foundation, and the Juvenile Diabetes Foundation (PWM & LMG), and National Institutes of Health Grant HL/AM-27120 (LMG). LMG, PWM, and MDH received financial support from California Metabolic Research Foundation, La Jolla, CA 92037.

References

1. Barber, A.J., Jamieson, G.A. 1970. Isolation and characterization of plasma membranes from human blood platelets. *J. Biol. Chem.* **245**:6357–6365
2. Bashford, C.L., Morgan, C.G., Radda, G.K. 1976. Measurement and interpretation of fluorescence polarization in phospholipid dispersions. *Biochim. Biophys. Acta* **426**:157–172
3. Berlin, E., Matusik, E.J., Young, C. 1980. Effect of dietary fat on the fluidity of platelet membranes. *Lipids* **15**:604–608
4. Butler, K.W., Tattrie, N.H., Smith, I.C.P. 1974. The location of spin probes in two phase mixed lipid systems. *Biochim. Biophys. Acta* **363**:351–360
5. Curtain, C.C., Gordon, L.M. 1983. ESR spectroscopy of membranes. *In*: Receptor Biochemistry and Methodology. J.C. Venter and L. Harrison, editors. Vol 1, Chapter 11. Alan R. Liss, New York (*in press*)
6. Curtain, C.C., Looney, F.D., Marchalonis, J.J., Raison, J.K. 1978. Changes in lipid ordering and state of aggregation in lymphocyte plasma membranes after exposure to mitogens. *J. Membrane Biol* **44**:211–232
7. Demel, R.A., Jansen, J.W.C.M., Dijck, P.W.M. van, Deenen, L.L.M. van 1977. The preferential interaction of cholesterol with different classes of phospholipids. *Biochim. Biophys. Acta* **465**:1–10
8. Dijck, P.W.M. van 1979. Negatively-charged phospholipids and their position in the cholesterol affinity sequence. *Biochim. Biophys. Acta* **555**:89–101
9. Elias, P.M., Goerke, J., Friend, D.S. 1978. Freeze-fracture identification of sterol-digitonin complexes in cell and liposome membranes *J. Cell Biol.* **78**:577–596
10. Gear, A.R.L. 1982. Rapid reactions of platelet studied by a quenched flow approach: Aggregation kinetics. *J. Lab. Clin. Med.* **100**:866–886
11. Gordon, L.M., Sauerheber, R.D. 1977. Studies on spin-

labelled egg lecithin dispersions. *Biochim. Biophys. Acta* **466**:34–43
12. Gordon, L.M., Sauerheber, R.D. 1982. Calcium and membrane stability. *In*: The Role of Calcium in Biological Systems. L.J. Anghileri and A.M. Tuffet-Anghileri, editors. Vol. 2, pp. 3–16. CRC Press, Boca Raton, Fla.
13. Gordon, L.M., Sauerheber, R.D., Esgate, J.A. 1978. Spin-label studies on rat liver and heart plasma membranes: Effects of temperature, calcium and lanthanum on membrane fluidity. *J. Supramol. Struct.* **9**:299–326
14. Gordon, L.M., Sauerheber, R.D., Esgate, J.A., Marchmont, R.J., Dipple, I., Houslay, M.D. 1980. The increase in bilayer fluidity of rat liver plasma membranes achieved by the local anesthetic benzyl alcohol affects the activity of intrinsic membrane enzymes. *J. Biol. Chem.* **255**:4519–4527
15. Higgins, J.A., Florendo, N.T., Barrnett, R.J. 1973. Localization of cholesterol in membranes of erythrocyte ghosts. *J. Ultrastruct. Res.* **42**:66–81
16. Houslay, M.D., Dipple, I., Gordon, L.M. 1981. Phenobarbital selectively modulates the glucagon-stimulated adenylate cyclase activity by depressing the lipid phase separation in the outer half of the bilayer of liver plasma membranes. *Biochem. J.* **197**:675–681
17. Houslay, M.D., Gordon, L.M. 1983. The activity of adenylate cyclase is regulated by the nature of its lipid environment. *In:* Membrane Receptors – Current Topics in Membranes and Transport. A. Kleinzeller and B.R. Martin, editors. Vol. 18, pp. 179–231. Academic Press, New York
18. Houslay, M.D., Metcalfe, J.C., Warren, G.B., Hesketh, T.R., Smith, G.A. 1976. The glucagon receptor of rat liver plasma membranes can couple to adenylate cyclase without activating it. *Biochim. Biophys. Acta* **436**:489–494
19. Houslay, M.D., Palmer, R.W. 1978. Changes in the form of Arrhenius plots of the activity of glucagon-stimulated adenylate cyclase and other hamster liver plasma membrane enzymes occurring on hibernation. *Biochem. J.* **174**:909–919
20. Houslay, M.D., Stanley, K.K. 1982. Dynamics of Biological Membranes. pp. 1–330. Wiley, New York
21. Hui, S.W., Parsons, D.F. 1976. Phase transitions of plasma membranes of rat hepatocytes and hepatoma cells by electron diffraction. *Cancer Res.* **36**:1918–1922
22. Jain, M.K., White, H.B. 1977. Long-range order in biomembranes. *Adv. Lipid Res.* **15**:1–60
23. Lee, A.G. 1975. Fluorescence studies on chlorophyll A incorporated into lipid mixtures, and the interpretation of "phase" diagrams. *Biochim. Biophys. Acta* **413**:11–23
24. Lee, A.G. 1977. Lipid phase transitions and phase diagrams. Mixtures involving lipids. *Biochim. Biophys. Acta* **472**:285–344.
25. Linhardt, K., Walter, K. 1965. Phosphatases (phosphomonoesterase). *In:* Methods of Enzymatic Analysis. H. Bergmeyer, editor. pp. 779–783, Academic Press, New York
26. Livingstone, C.J., Schachter, D. 1980. Lipid dynamics and lipid-protein interactions in rat hepatocyte plasma membranes. *J. Biol. Chem.* **255**:10902–10908
27. Sandermann, H. 1978. Regulation of membrane enzymes by lipids. *Biochim. Biophys. Acta* **515**:209–237
28. Sauerheber, R.D., Gordon, L.M., Crosland, R.D., Kuwahara, M.D. 1977. Spin-label studies on rat liver and heart plasma membranes: Do probe-probe interactions interfere with the measurement of membrane properties? *J. Membrane Biol.* **31**:131–169
29. Sauerheber, R.D., Zimmerman, T.S., Esgate, J.A., Vanderlaan, W.P., Gordon, L.M. 1980. Effects of calcium, lanthanum and temperature on the fluidity of spin-labeled human platelets. *J. Membrane Biol.* **52**:201–219
30. Shattil, S.J., Cooper, R.A. 1976. Membrane microviscosity and human platelet functions. *Biochemistry* **15**:4832–4837
31. Steiner, M. 1981. Vitamin E changes the membrane fluidity of human platelets. *Biochim. Biophys. Acta* **640**:100–105
32. Verma, S.P., Wallach, D.F.H. 1975. Evidence for constrained lipid mobility in the erythrocyte ghost. A spin label study. *Biochim. Biophys. Acta* **382**:73–82
33. Whetton, A.D., Gordon, L.M., Houslay, M.D. 1983. Elevated membrane cholesterol levels inhibit glucagon-stimulated adenylate cyclase activity. *Biochem. J.* **210**:437–449

Received 11 January 1983; revised 14 April 1983